*Cerebral Cortex*, August 2020;30: 4677–4688

**doi: 10.1093/cercor/bhaa073**
Advance Access Publication Date: 20 March 2020
Original Article



ORIGINAL ARTICLE

# Confidence in Decision-Making during Probabilistic Tactile Learning Related to Distinct Thalamo–Prefrontal Pathways

Bin A. Wang[1,2] and Burkhard Pleger[1,2,3]

[1]Department of Neurology, BG University Hospital Bergmannsheil, Ruhr University Bochum, 44789 Bochum, Germany, [2]Collaborative Research Centre 874 "Integration and Representation of Sensory Processes", Ruhr University Bochum, 44780 Bochum, Germany and [3]Department of Neurology, Max Planck Institute for Human Cognitive and Brain Sciences, 04103 Leipzig, Germany

Address correspondence to Burkhard Pleger, Department of Neurology, BG University Hospital Bergmannsheil, Ruhr University Bochum, Bürkle-de-la-Camp Place 1, 44789 Bochum, Germany. Email: Burkhard.V.Pleger@ruhr-uni-bochum.de.

## Abstract

The flexibility in adjusting the decision strategy from trial to trial is a prerequisite for learning in a probabilistic environment. Corresponding neural underpinnings remain largely unexplored. In the present study, 28 male humans were engaged in an associative learning task, in which they had to learn the changing probabilistic strengths of tactile sample stimuli. Combining functional magnetic resonance imaging with computational modeling, we show that an unchanged decision strategy over successively presented trials related to weakened functional connectivity between ventralmedial prefrontal cortex (vmPFC) and left secondary somatosensory cortex. The weaker the connection strength, the faster participants indicated their choice. If the decision strategy remained unchanged, participant's decision confidence (i.e., prior belief) was related to functional connectivity between vmPFC and right pulvinar. While adjusting the decision strategy, we instead found confidence-related connections between left orbitofrontal cortex and left thalamic mediodorsal nucleus. The stronger the participant's prior belief, the weaker the connection strengths. Together, these findings suggest that distinct thalamo–prefrontal pathways encode the confidence in keeping or changing the decision strategy during probabilistic learning. Low confidence in the decision strategy demands more thalamo–prefrontal processing resources, which is in-line with the theoretical accounts of the free-energy principle.

**Key words:** decision-making, prior belief, tactile learning, thalamo–prefrontal connection

## Introduction

In a probabilistic environment, changes in the statistical structure of the world introduce uncertainty in the prediction of sensory inputs. Making inference about the causes of this uncertain information based on previous experience is the fundament of perceptual learning. Such inference is crucial for cognitive flexibility and hence the prerequisite for sharpening sensory precision and accelerating motor reactions to sensory target events through learning (Bestmann et al. 2008; den Ouden et al. 2010; van Ede et al. 2010, 2014; Vossel et al. 2015).

According to the predictive coding (PC) principle, sensory systems operate the inference of the causes of sensory inputs under hierarchical Bayesian principles (Friston 2005). The central postulate of the Bayesian perspective is that the brain continuously updates a hierarchical generative model based on prior experience to predict future events and infer on the causal structure of the world. Prediction errors, indexing the discrepancy between the expected and actual outcome, serve to update prior belief, which, in turn, guides the direction of subsequent decision-making (Friston 2005; Clark 2013). This belief updating process

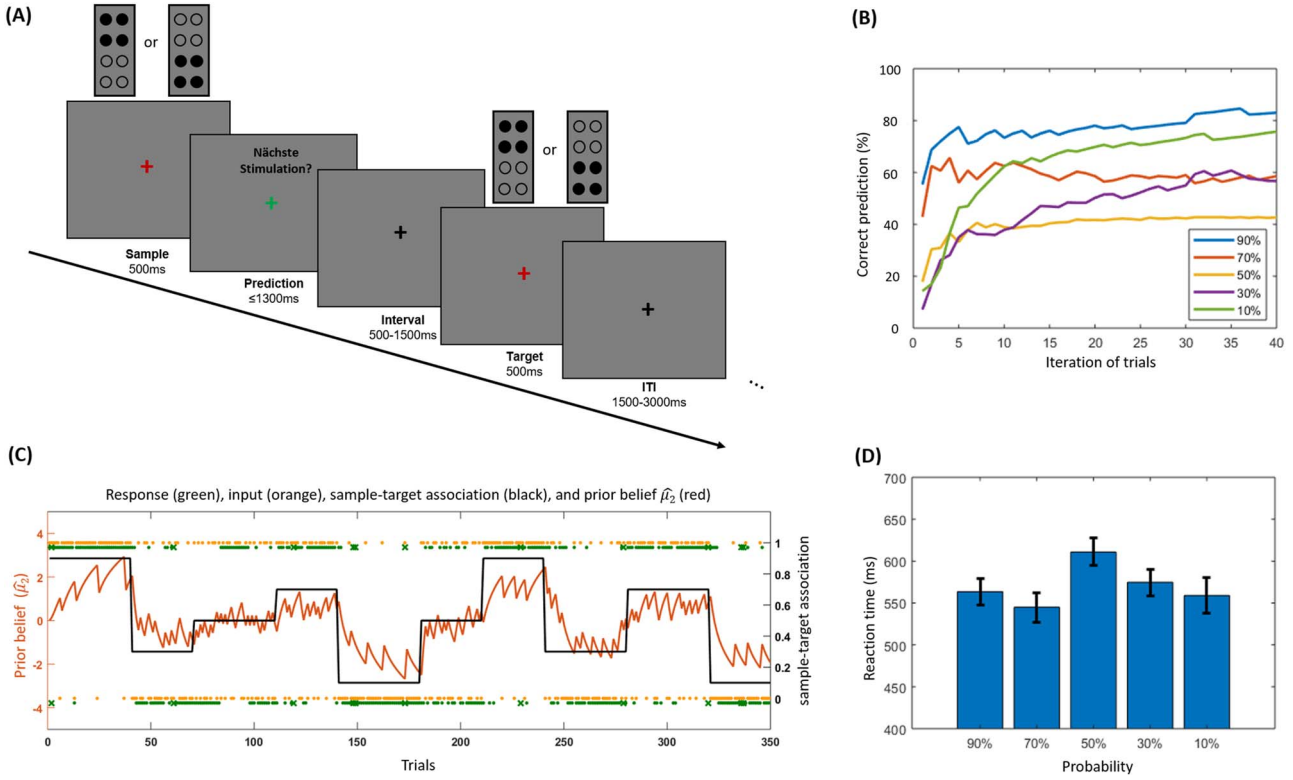


**Figure 1.** Illustration of the experimental design and participants' behavioral performance. (*A*) Task design. Participants were instructed to predict the target stimulus as fast and accurately as possible based on how much they believed that the sample tactile stimulus matches the target (sample–target association). (*B*) The proportion of correctly predicted trials over time for each of the five sample–target associations (i.e., 90%, 70%, 50%, 30%, and 10%). Increases in correct predictions over time for the different predictabilities indicate successful learning of sample–target associations. (*C*) Subject-specific example of prior belief ($\hat{\mu}_2$) and how it changed over the five sample–target associations. Black line: sample–target associations consisted of strongly predictive (90% and 10%), moderately predictive (70% and 30%), and nonpredictive (50%) blocks. We always presented two blocks for each of the five sample–target associations. Red line: example of a subject-specific trajectory of prior belief across the different sample–target associations. Orange dots: trial outcomes (or tactile inputs). Green dots: observed responses. Green cross: participant's missing responses. (*D*) The mean reaction time for the five sample–target associations. The error bar depicts the standard deviation. Reaction times were significantly longer in blocks with no predictability (i.e., 50%) than in blocks with strong (i.e., 90% and 10%) or moderate predictability (i.e., 70% and 30%).

rests on multiple prediction errors at different hierarchical levels, for example, probabilistic associations of sensory events and how they change over time (Behrens et al. 2007).

In the tactile domain, bottom-up prediction errors are well reflected by neural activity along the whole somatosensory pathway, not only involving the primary (S1) and secondary (S2) somatosensory cortex but also the thalamus (Allen et al. 2016; Fardo et al. 2017). The integration of the afferent thalamic volley with top-down control signals arising in the prefrontal and cingulate cortex seems responsible for updating prior belief in light of the preceding prediction error (Seth et al. 2012; Seth 2013; Allen et al. 2016; Fardo et al. 2017). Despite all this evidence, it remains to be established how prior belief is encoded and how it allows the brain to quickly and flexibly generate decisions during perceptual learning.

The prediction-error–related adjustment of the decision strategy—the subject's internal rule to decide whether or not the statistical property of the environment has been changed—seems to relate to certain shifts in functional connectivity, for instance, between the sensory and motor cortex (den Ouden et al. 2010). Projections between the ventralmedial prefrontal cortex (vmPFC) and sensory cortices appear to mediate changes in perceptual awareness, whereas connections between vmPFC and the orbitofrontal cortex (OFC) were shown to be involved in signaling changes in the value assigned to the sensory stimulus (Howard et al. 2016). Prefrontal pathways seem to also support the formation of a perceptual or associative representation of the sensory stimulus, which is a crucial prerequisite for decisions based on perceptual evidence (Rushworth et al. 2011; Bari et al. 2019). Prefrontal projections to the thalamus, especially to its mediodorsal nucleus (MD), were recently found to encode predictive cues, highlighting the thalamus' potential role in mediating the necessary cognitive flexibility for decision-making in an probabilistic environment (Mitchell 2015; Otis et al. 2017; Marton et al. 2018; Nakayama et al. 2018).

Based on this evidence, we hypothesized that during tactile learning, the flexibility in changing the decision strategy is related to activity in prefrontal cortex, such as vmPFC and OFC. We further expected that these prefrontal regions interact with regions at the crossroad between cognitive and sensory processing, such as the thalamus, to represent the strength of prior belief. To address these hypotheses, we used a tactile associative learning task where participants had to learn the predictive strength of a sample stimulus and explicitly predict the target stimulus before receiving it (Fig. 1A), which was described in a previously conducted study (Wang et al. 2020). Our task allowed us to investigate the flexibility in decision-making through disentangling the adjustment of the decision strategy (*Change*: all trials "$n+1$" decided in a different way as the preceding trial "$n$"), from those trials where the decision

strategy did not change (*Keep*: all trials "$n+1$" decided in the same way as the preceding trial "$n$"). We combined computational modeling with functional magnetic resonance imaging (fMRI) to investigate the neurophysiological processes underlying the modulation of prior belief for an adjusted or unchanged decision strategy. Using fMRI, we first isolated those prefrontal brain regions whose activity represents the adjustment of the decision strategy (*Change*) or an unchanged decision strategy (*Keep*). Next, we identified prefrontal connectivity to the thalamus in relation to the strength of prior belief for both decision strategies.

## Materials and Methods

### Participants

Thirty-three healthy male participants (mean age ± SD: 25.1 ± 3.8 years) were recruited. We only employed male participants to exclude influences of hormonal fluctuations over the menstrual cycle on learning and associated blood-oxygen-level–dependent (BOLD) signals (Dreher et al. 2007; Sacher et al. 2013; Wetherill et al. 2016). Participants with more than 20% invalid trials or less than 60% correct responses were excluded from further analyses. According to these criteria, five participants were excluded, and the data of 28 participants were further analyzed (mean age ± SD: 25.3 ± 3.9 years). All participants were right-handed and had normal or corrected to normal vision. A history of psychiatric or neurological disorders as well as any regular medication was exclusion criteria. The study was approved by the local ethics committee of the Ruhr University Bochum. All participants gave written informed consent prior to participation.

### Tactile Stimuli

The tactile stimuli were generated and delivered using an MRI-compatible Braille device (Metec, Stuttgart, Germany). The device consisted of eight plastic pins, aligned in two series of four pins (pin diameter 1.2 mm, rounded top, interpin spacing 2.45 mm). We applied two alternative tactile stimulation patterns: either the upper four pins (distal) were raised and the lower four pins (proximal) were lowered (i.e., Upper) or vice versa (i.e., Lower). Stimuli were applied to the index fingertip of the right (dominant) hand. The Braille device was controlled using Presentation software (version 20.1, Neurobehavioral Systems) through Metec Virtual Braille Device by TCP-IP commands. To ensure that both tactile stimulation patterns were perceived correctly, participants performed a tactile detection test prior to the training and MRI session. During the test run, participants had to report which pattern they received until they perceived and distinguished both tactile stimulation patterns 100% correctly.

### Experimental Design

We employed a tactile associative learning task where participants were instructed to learn the predictive strength of tactile sample stimuli in forecasting subsequently presented target stimuli (Fig. 1A). In each trial, participants first received one out of the two sample stimuli (Upper or Lower) for 500 ms. A red fixation cross was simultaneously presented on the screen via fMRI-compatible LCD goggles (Visuastim Digital, Resonance Technology Inc.). Participants were instructed to maintain central fixation during tactile stimulation. Following the sample, the red fixation cross turned green, and participants had to press one out of two buttons (LumiTouch keypads, Photon Control Inc.) with the index or middle finger of the left hand to indicate which of the two target stimuli (Upper or Lower) may follow. Participants responded by pressing the "up" or the "down" button. The up button corresponded to the upper pattern and the down button to the lower pattern. Participants were instructed to indicate their prediction by pressing the button within 1300 ms as quickly and accurately as possible. They were told to learn the predictability of the sample and to use the information given by the sample to adjust their prediction accuracy, rather than to predict randomly. After the button press and a short interval of 500–1500 ms, the target stimulus (Upper or Lower) was presented for 500 ms. Trials were presented with randomized intertrial interval ranging between 1500 and 3000 in 100 ms steps.

The predictability of the sample was manipulated by modulating the strength of the sample–target association over time. The task consisted of strongly predictive (90% and 10%), moderately predictive (70% and 30%), and nonpredictive (50%) blocks. In blocks with 90% and 70% predictability, the sample matched the target in 90% and 70% of trials, respectively, while the sample mismatched the target in 90% and 70% of trials in blocks with 10% and 30% predictability (i.e., reversal learning). In blocks with 50% predictability, the number of matches and mismatches was the same, and trials were presented randomly. The whole experiment comprised 10 blocks in total—two blocks for each sample–target association. One block consisted of an equal number of the two tactile patterns, presented in random order. The sequence of blocks was pseudorandomized and fixed across participants to ensure intersubject comparability of the associated learning processes (Iglesias et al. 2013; Vossel et al. 2014). Participants were informed that the sample–target association would change over time, but the exact probabilities (i.e., 90%/10%, 70%/30%, and 50%) were unknown to the participant. To avoid the prediction of a new block onset, blocks were presented pseudorandomly, and the two blocks for each sample–target association were once presented with 30 trials and the other time with 40 trials (Fig. 1C). The fMRI experiment consisted of 350 trials, which we split into three runs, each lasted ~10 min, resulting in a total scanning time of 30 min.

To enhance motivation throughout the experiment, we offered a monetary reward of 1€ added to the general reimbursement (5€/run) for a 5% increase in correct predictions in each fMRI run. After each run, the participants were given a visual feedback (10s) about how many trials they correctly or incorrectly predicted, how many were missed, and how much money they made during the preceding run.

### Analyses of Behavioral Data

Trials with missed responses or excessively long reaction time (>1300 ms) were excluded from further analyses (2.9 ± 0.6% SEM of all trials). To assess whether the sample–target associations were learned, we applied the proportion of correct predictions across the different sample–target associations to the within-subject one-way ANOVA. Bonferroni-corrected posthoc paired *t*-tests were used to assess whether the proportion of correct predictions in learning blocks (i.e., 90%/70%/30%/10%) were significantly different from control blocks (i.e., 50%). In addition, we also tested reaction times across the different sample–target associations using the within-subject one-way ANOVA.

Next, we examined the neural substrates related to the flexibility in decision-making across all sample–target associations.

To this end, the present task encompassed two types of trials based on participants' decisions: 1) the adjustment of the decision strategy (*Change*: all trials "$n+1$" decided in a different way as the preceding trial "$n$") and 2) trials in which the decision strategy did not change (*Keep*: all trials "$n+1$" decided in the same way as the preceding trial "$n$").

Behavioral data were applied to an hierarchical Gaussian filter (HGF) as implemented in the HGF v5.2 toolbox (https://www.tnu.ethz.ch/de/software/tapas.html), to calculate the individual differences in the trial-wise estimation of prior belief about the external states on different levels (Mathys et al. 2011; Iglesias et al. 2013; Vossel et al. 2014; Kuhns et al. 2017; Weilnhammer et al. 2018). The HGF consists of a perceptual and a response model, which describes a framework where an agent receives a sequence of inputs (stimuli) and generates behavioral responses based on perceptual inference (Mathys et al. 2011). The perceptual model comprised three levels of inference about the external states: The first level represented the tactile observation in each trial, $\chi_1(t)$. In our study, it was represented by a binary input, with $\chi_1(t)=1$ for the target matched the sample and $\chi_1(t)=0$ for the target mismatched the sample. The second level $\chi_2(t)$ represented the sample–target association, that is, the probability that the target matched the sample ($\chi_1(t)=1$). The probability distribution of $\chi_1(t)=1$ was a Bernoulli distribution, determined by higher-level $\chi_2(t)$ through sigmoid transformation. The value of $\chi_2(t)$ was based on the previous trial ($t-1$) and changed from trial to trial as a Gaussian random walk. The changing rate of $\chi_2(t)$ was determined by both, the third level $\chi_3(t)$ and a subject-specific parameter $\omega_2$. The third level, $\chi_3(t)$, represented the stability of tactile perception (i.e., how fast $\chi_2(t)$ changed from trial to trial). The step size of Gaussian random walk on the third level $\chi_3(t)$ was determined by a second subject-specific parameter $\omega_3$. So, the variance of these environmental hidden states depended on the state at the next higher-level changing as a Gaussian random walk. Subject-specific parameters $\omega_2$ and $\omega_3$ were estimated from individual responses using a unit square sigmoid model (response model). In the present study, we focused on the absolute value of $\hat{\mu}_2^{(t)}$ at the second level of the model, which was prior belief about the sample–target association before experiencing the target stimulus. Here, we provide a brief description of the nature of this quantity: prior belief evolved from posterior belief of the previous trial ($\mu_2^{(t-1)}$). Similar to classical reinforcement or associative learning models, such as the Rescorla–Wagner learning model (Rescorla and Wagner 1972), the posterior belief ($\mu_2^{(t)}$) about the sample–target association was updated after each trial based on the prediction error or the difference between the expected and received outcome. Updating prior belief was described by the following equation:

$$\mu_2^{(t)} = \hat{\mu}_2^{(t)} + \psi_2^{(t)}\delta_1^{(t)}$$

$$\hat{\mu}_2^{(t)} = \mu_2^{(t-1)},$$

where $\delta_1$ was the prediction error, indexing the difference between the actual and the predicted outcome on trial $t$ at the first level ($\mu_1^{(t)} - \hat{\mu}_1^{(t)}$). $\psi_2$ indicated the precision of prediction. The precision weight ($\psi_2$) was updated with every trial, so that it can be considered as the equivalence of a dynamic learning rate in reward learning models (Preuschoff and Bossaerts 2007; Mathys et al. 2011).

## FMRI Data Acquisition and Preprocessing

FMRI was conducted with a Philips 3.0 T Achieva X-series scanner using a 32-channel head coil. We used a $T_2*$-weighted echo-planar imaging sequence (voxel size, $2\times2\times3$ mm; field of view 224 mm; interslice gap, 0.6 mm; TR = 2800 ms; TE = 36 ms) for functional imaging and acquired 36 transaxial slices parallel to the anterior–posterior commissure (AC–PC) with interleaved slice acquisition covering the whole brain. As anatomical reference, high-resolution $T_1$-weighted images were acquired using an isotropic $T_1$ TFE sequence (voxel size: $1\times1\times1$ mm$^3$, field of view 240 mm) with 220 transversally oriented slices covering the whole brain.

Across the three fMRI runs, we acquire a total of 644 EPI volumes. To allow for $T_1$-equilibration, five dummy scans preceded data acquisition in each run. These scans were removed before further processing. Data were pre- and postprocessed with the Statistical Parametric Mapping software SPM12 (Wellcome Department of Imaging Neuroscience, University College London, UK; http://www.fil.ion.ucl.ac.uk/spm) running in the Matlab R2017b (MathWorks Inc.) environment. For preprocessing, images were applied to slice time correction, spatial realignment, and normalization to the MNI template using the unified segmentation approach (Ashburner and Friston 2005). Finally, normalized images were spatially smoothed using a Gaussian filter with a full-width half-maximum kernel of 8 mm. We tested the effect of kernel size on our findings and reanalyzed the data using 6 mm instead of 8-mm smoothing. We found that the results resembled those of our analyses with 8-mm smoothing (please see supplementary material, Supplementary Figs 1–3, and Supplementary Table 1 for more details).

## General Linear Modeling of fMRI Data

The general linear model (GLM) in SPM 12 was used to analyze fMRI data. For each participant, we conducted a first-level GLM. Events were time-locked to the onset of the presentation of the sample stimulus using stick functions and split into two regressors, one for *Keep* and the other one for *Change* trials. For each of these two regressors, the absolute value of trial-by-trial prior belief ($|\hat{\mu}_2^{(t)}|$) was defined as a parametric modulator (see Supplementary Fig. 4 for an example of GLM design matrix). Onsets were convolved with the canonical hemodynamic response function in an event-related fashion. Regressors of no interest included the presentation of the target stimuli (all trials collapsed to a single regressor), invalid trials (i.e., missing or late responses), and the six head motion parameters as estimated during the realignment procedure. Data were high-pass filtered at 1/128 Hz.

Using the GLM, we investigated neural mechanisms underlying either the adjustment of the decision strategy (*Change*) or an unchanged decision strategy (*Keep*) (not accounting for prior belief). To this end, the contrasts "*Keep* > *Change*" and "*Keep* < *Change*" were applied to the group-level one-sample t-test. Analyses were thresholded at $P<0.05$ familywise error (FWE)–corrected for the whole brain. We also compared prior belief-related parametric effects between *Keep* and *Change* by applying the same contrasts described above to the GLM regressors representing the parametric modulation of *Keep* and *Change* by trial-by-trial prior belief. Individual contrast images were again applied to the group level one-sample t-test and thresholded at $P<0.05$, FWE-corrected for the whole brain.

### Psychophysiological Interaction

Psychophysiological interaction (PPI) was used to assess context-related differences in functional connectivity between a given seed region and the rest of the brain (Friston et al. 1997). Because our results revealed that different PFC regions, that is, vmPFC and OFC, were involved in *Keep* and *Change*, respectively, we applied two PPIs, one using the vmPFC as the seed and the other one using OFC as the seed. Individual time series of each seed region were extracted from ROIs that were selected from the nearest local maximum of the contrast of interest (i.e., vmPFC seed region, *Keep* > *Change*; OFC seed region, *Change* > *Keep*) within a radius of 12 mm from the group maximum. The first Eigenvariate was then calculated across all voxels surviving $P = 0.05$ uncorrected, within a 6-mm sphere centered on the individual peak voxel. The resulting BOLD time series were adjusted for effects of no interest (e.g., target periods, invalid trials, and movement parameters) and deconvolved to generate time series required for constructing first-level GLMs for the PPIs.

The standard PPI analysis implemented in SPM is used to assess connectivity differences between task conditions of interest (psychological variable) and their interaction with neural activity (physiological variable). In our case, the psychological variable of interest is itself an interaction—an interaction between conditions (*Keep* and *Change*) and prior belief derived from HGF. This means that we were effectively testing for a three-way interaction between a physiological (time series of the seed region) and two psychological variables (conditions and prior belief). Compared with the standard PPI implemented in SPM, the generalized form of context-dependent PPIs (gPPIs) allows to model more than two conditions and multiple PPI terms (McLaren et al. 2012). Empirical evidence emphasizes that gPPI improves flexibility of statistical modeling, model fit, specificity to true negative findings, and sensitivity to true positive findings. Therefore, PPI analyses were performed with the gPPI Toolbox (McLaren et al. 2012) to assess changes in connectivity between *Keep* and *Change*.

The PPI GLM at the single-subject level contained nine regressors: four regressors representing *Keep* and *Change*, as well as their parametric trial-by-trial modulation by prior belief ($|\hat{\mu}_2^{(t)}|$), four PPI regressors representing the interactions between the physiological variable (i.e., time series of the seed region) and *Keep* and *Change*, as well as their parametric modulation by prior belief. The last regressor represented the physiological variable. Regressors of no interest included the presentation of the target stimuli, invalid trials, and the six head motion parameters (see Supplementary Fig. 5 for an example of PPI GLM design matrix).

First, we examined general changes in connectivity between *Keep* and *Change* trials (not accounting for prior belief). To this end, first-level contrast images were created using the PPI regressor of the interaction between the physiological variable and *Keep* trials, as well as the interaction between the physiological variable and *Change* trials. The contrast images (i.e., "*Keep* > *Change*" and "*Keep* < *Change*") were next applied to the group-level one-sample *t*-test and thresholded at $P = 0.05$, FWE-corrected. We hypothesized, that the adjustment of the decision strategy (*Change*) as well as an unchanged decision strategy (*Keep*) were related to functional connections between the PFC and brain regions involved in tactile perception, including S1, S2, and specifically bilateral thalamus. That is why we performed small-volume correction (SVC) by restricting the search volume to S1, S2, and both thalami. To this end, we created a brain mask including the cytoarchitectonic maps of bilateral S1, S2, and thalamus, as implemented in the SPM Anatomy Toolbox (Eickhoff et al. 2005; Zaborszky et al. 2008).

In order to assess prior belief-related connectivity, we next conducted a three-way interaction between the physiological (i.e., BOLD signal in the seed region) and two psychological variables (i.e., trial conditions and prior belief). We obtained first-level contrast images using the PPI regressor of the parametric modulator, representing the interaction between the physiological variable and its parametric modulation by prior belief. The three-way interaction contrast images between *Keep* and *Change* (i.e., PPI regressor *Keep* > *Change* by prior belief and PPI regressor *Change* > *Keep* by prior belief) were then applied to the group-level one-sample *t*-test and thresholded at $P = 0.05$, FWE-corrected. Accumulating evidence suggests that functional connectivity between the prefrontal cortex and distinct thalamic nuclei encode behavioral flexibility and action–outcome associations during learning and decision-making (Mitchell 2015; Otis et al. 2017; Marton et al. 2018; Nakayama et al. 2018; Parnaudeau et al. 2018; Fresno et al. 2019). Based on this evidence, we hypothesized to identify connections between prefrontal cortex and the thalamus in relation to the strength of prior belief for both, the adjustment of the decision strategy (*Change*) and an unchanged decision strategy (*Keep*). To this end, we performed SVCs by restricting the search volume to the thalamus. To this end, we created a mask covering bilateral thalamus as offered by the SPM Anatomy Toolbox (Eickhoff et al. 2005; Zaborszky et al. 2008).

Since this three-way interaction did not reveal any prior belief-associated significant results surviving FWE-corrected thresholding at $P = 0.05$, we next applied the averaged strength of individual prior belief to a group-level regression analysis in SPM to assess the mean prior belief-related connectivity across participants for *Keep* and *Change* trials separately. For the *Keep* condition, analysis was complemented using the vmPFC coupling strength (i.e., PPI parameters for *Keep*) as dependent variable and the strength of individual prior belief in the *Keep* condition as a covariate. For the *Change* condition, we performed group-level regression analysis using the OFC coupling strength (i.e., PPI parameters for *Change*) as dependent variable and the strength of individual prior belief in the *Change* condition as a covariate. We again applied SVC together with FWE correction thresholded at $P = 0.05$ to assess associated effects in the thalamus.

## Results

### Behavioral Results

The proportion of missing responses was 2.19% (±0.53 SEM). They were excluded from further analysis of behavioral data and were modeled separately in the GLM analyses of the imaging data. Figure 1B shows increases in proportion of correct predictions for the different sample–target associations over time. Please note that participants' performance in the blocks at chance level was below 50% (i.e., 43%). The most likely explanation for this is that participants kept using the strategy learned in the previous block (i.e., 90% or 70%) during the first trials of each chance block. This explanation is supported by our data. Performance during the first half of trials in chance blocks was in fact far below chance level (41%), whereas in the second half performance increased to 45%.

To test whether sample–target associations (90%/70%/50%/30%/10%) were learned, we analyzed the proportion of correct

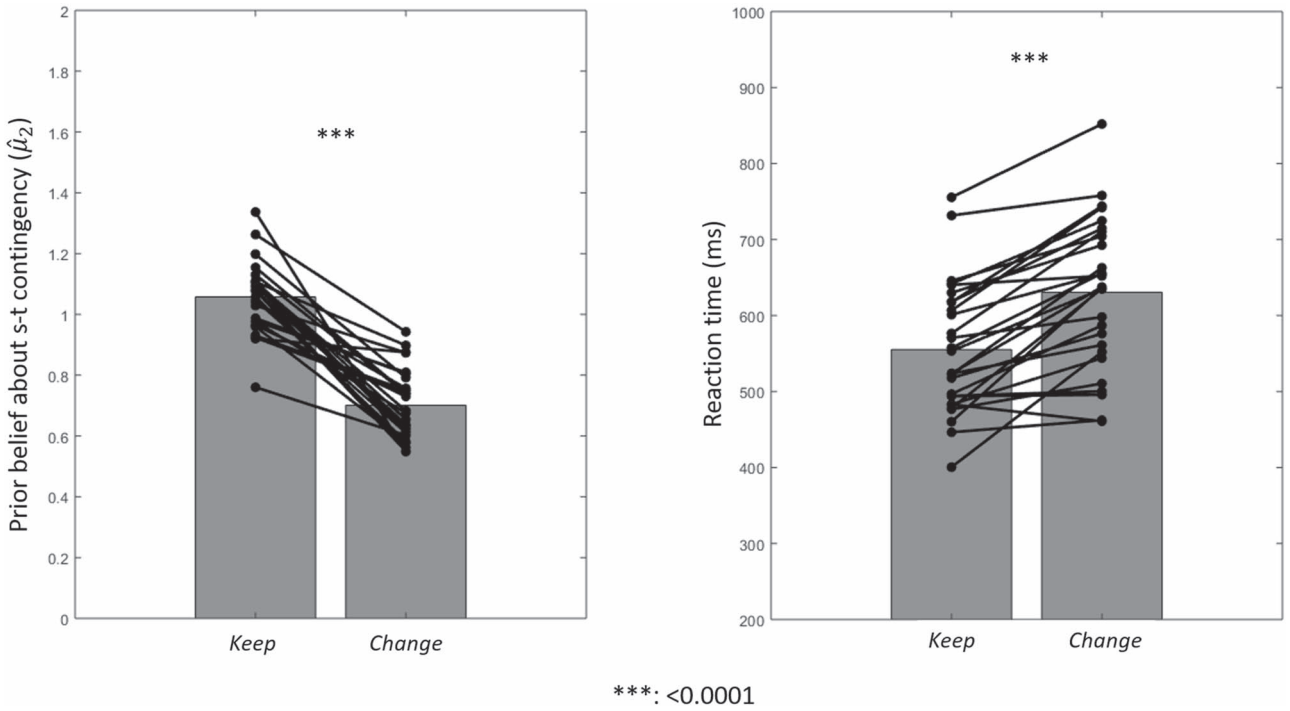


**Figure 2.** The comparison of individual prior beliefs (left) and reaction time (right) between *Keep* (trials "$n+1$" decided in the same way as the preceding trial "$n$") and *Change* (trials "$n+1$" decided in a different way as the preceding trial "$n$"). The bar indexes the mean, and black lines connect the two data points of each participant. *** indicates threshold $P < 0.0001$.

predictions in a one-way repeated measures ANOVA. This ANOVA revealed a significant effect of learning ($F(4,27) = 256$, $P < 0.001$). Posthoc paired *t*-tests showed significantly more correct predictions in learning blocks with high predictability (i.e., 90%/10%) as compared with blocks with low predictability (i.e., 70%/30%, $t(1,27) = 20.75$, $P < 0.001$, Bonferroni-corrected) and unpredictable blocks (i.e., 50%, $t(1,27) = 24.70$, $P < 0.001$, Bonferroni-corrected). We also tested reaction times across sample–target associations (Fig. 1D). We found that the reaction time was significantly longer in blocks with targets that were unpredictable (i.e., 50%) than in blocks with strong (i.e., 90%/10%, $t(1,27) = 4.52$, $P < 0.001$, Bonferroni-corrected) or moderate predictability (i.e., 70%/30%, $t(1,27) = 4.90$, $P < 0.001$, Bonferroni-corrected). Together, these findings suggest successful probabilistic learning.

To assess differences in prior belief ($|\hat{\mu}_2^{(t)}|$) derived from HGF and reaction times for *Keep* ($211 \pm 17$ trials) and *Change* ($122 \pm 10$ trials), we compared both parameters between both conditions. Figure 2 shows that prior belief was significantly stronger (left) and reaction times were significantly shorter (right) in *Keep* trials as compared with *Change* trials ($P < 0.0001$). Neither for *Keep* nor for *Change* we found a relationship between prior belief and reaction times ($P = 0.35$ for *Keep*, and $P = 0.56$ for *Change*).

## Neural Activations Associated with the Adjustment of the Decision Strategy (*Change*) or with an Unchanged Decision Strategy (*Keep*)

First, we investigated the different neural substrates related to either the adjustment of the decision strategy or an unchanged decision strategy by comparing *Keep* versus *Change* (not accounting for prior belief). Compared with the adjustment of the decision strategy, we observed the expected significant activation in vmPFC when participants did not change their decision strategy (*Keep* > *Change*). Furthermore, we identified the precuneus and bilateral gyri parahippcampalis in the same context ($P < 0.05$, FWE-corrected for the whole brain; Fig. 3A and Table 1). The adjustment of decision strategy (*Change* > *Keep*) entailed the expected significant activation in the left OFC. We also depicted significant effects for the adjustment of the decisions strategy in the left insula, bilateral inferior parietal cortex, dorsal premotor cortex (PMd), and supplementary motor area (SMA) ($P < 0.05$ FWE-corrected for the whole brain; Fig. 3B and Table 1). The comparison of prior belief-related parametric effects between *Keep* and *Change* did not reveal any significant effects.

## Differences in Functional Connectivity between the Adjustment of the Decision Strategy (*Change*) and an Unchanged Decision Strategy (*Keep*)

Next, we assessed differences in functional connectivity between *Keep* and *Change* using PPI analyses with either vmPFC or OFC as the seed region. According to our hypotheses, we applied SVC to assess potential effects along the somatosensory pathway constituted by the thalamus, S1, and S2.

Compared with the adjustment of the decision strategy, an unchanged decision strategy (i.e., contrast of PPI regressors *Keep* > *Change*) entailed a significantly weakened coupling between vmPFC and bilateral S2 (left S2: peak MNI coordinates x/y/z = −52/−30/18, $t(1,27) = 5.46$, $P = 0.017$, small-volume FWE-corrected; right S2: peak MNI coordinates x/y/z = 48/−26/16, $t(1,27) = 5.01$, $P = 0.046$, small-volume FWE-corrected, Fig. 4A). Differences in reaction times between *Keep* and *Change* (i.e.,

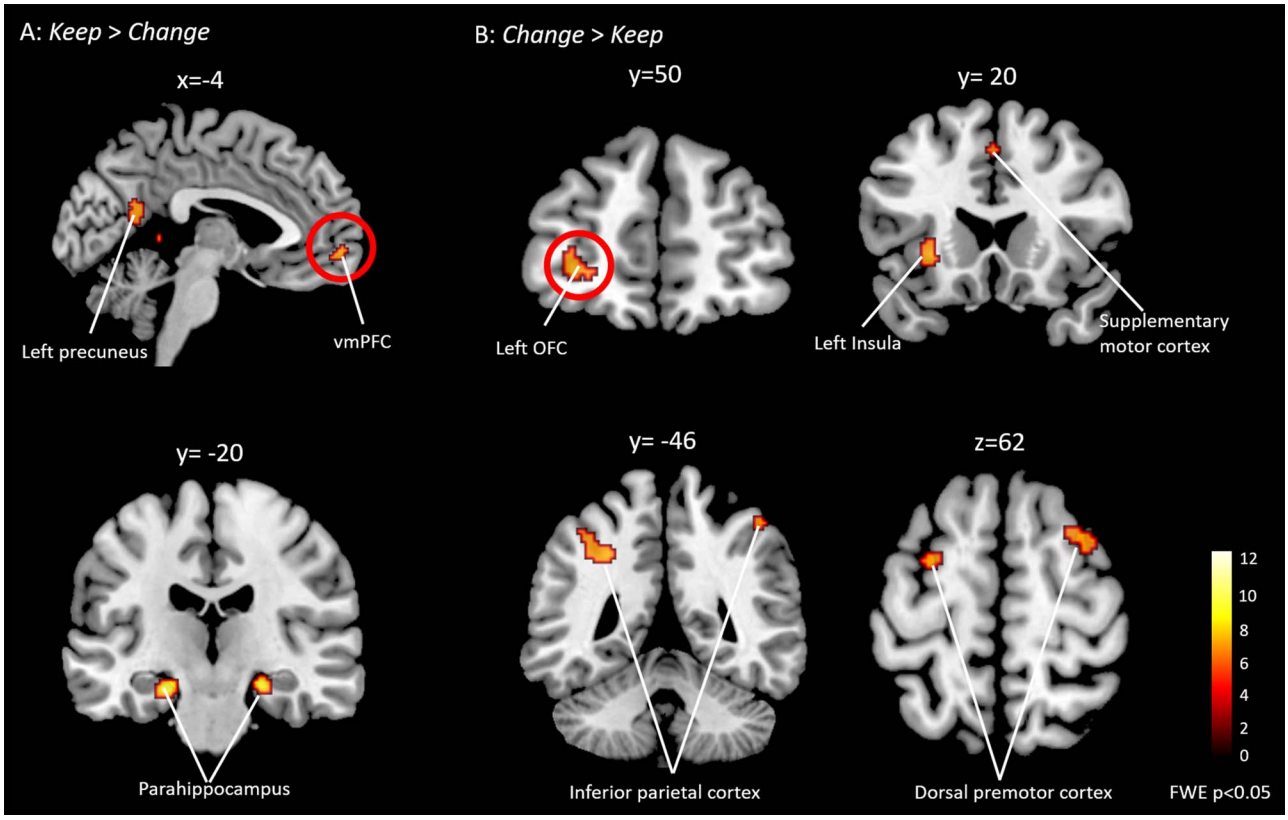


**Figure 3.** Brain regions related to the adjustment of the decision strategy (*Change* > *Keep*) or to an unchanged decision strategy (*Keep* > *Change*). Significant activations were obtained from the contrasts "*Keep* > *Change*" (*A*) and "*Change* > *Keep*" (*B*) (not accounting for prior belief). Significant activation ($P < 0.05$ FWE-corrected) were superimposed on sagittal, coronal, and axial slices of a standard $T_1$-weighted image as implemented in SPM. Coordinates above each slice index their location in MNI space. (*A*) If participants did not change their decision strategy, we observed activity in vmPFC, the precuneus, and bilateral parahippcampus. (*B*) Adjusting the decision strategy related to activity in left OFC, left insula, bilateral inferior parietal cortex, dorsal premotor cortex, and SMA (see Table 1 for MNI peak coordinates, cluster sizes, and *t*-scores). The regions surrounded by the red circle (vmPFC and OFC) were next used as seeds for connectivity analyses (i.e., PPI). Color coding indexes the *t*-scores in each voxel.

**Table 1** Brain regions related to the adjustment of the decision strategy (*Change*) or to an unchanged decision strategy (*Keep*)

| Regions | Hemisphere | Peak coordinates | | | Cluster size (in voxels) | *t*-score |
|---|---|---|---|---|---|---|
| | | x | y | z | | |
| *Keep* > *Change* | | | | | | |
| Ventral–medial frontal cortex | L and R | −2 | 60 | −4 | 46 | 7.00 |
| Precuneus | L | −10 | −50 | 6 | 209 | 7.97 |
| Parahippocampus | L | −22 | −22 | −16 | 86 | 9.50 |
| Parahippocampus | R | 22 | −20 | −14 | 38 | 9.00 |
| *Change* > *Keep* | | | | | | |
| Orbital frontal cortex | L | −30 | 52 | −2 | 76 | 7.35 |
| Insula | L | −30 | 24 | −2 | 81 | 7.25 |
| Premotor cortex | L | −28 | 0 | 64 | 29 | 6.82 |
| Premotor cortex | R | 30 | 10 | 62 | 36 | 6.56 |
| Supplementary motor area | L and R | 0 | 24 | 44 | 43 | 6.50 |
| Inferior parietal cortex | L | −32 | −50 | 42 | 183 | 7.53 |
| Inferior parietal cortex | R | 46 | −44 | 56 | 28 | 6.73 |

*Keep* minus *Change*) significantly correlated with difference in vmPFC-left S2 connectivity ($r = 0.378$, $P = 0.024$, Fig. 4B). We found no reaction time-related correlation with the connection strength to right S2, ipsilateral to the stimulated finger. Together, these findings suggest that the weaker the connectivity between vmPFC and left S2, the faster participants indicated their decisions. We did not find any correlation between connectivity strength and changes in the strength of prior belief. Using the OFC as a seed for PPI analysis, we found no significant effects while participants adjusted their decision strategy compared with an unchanged decision strategy (i.e., contrast of PPI regressors *Change* > *Keep*).

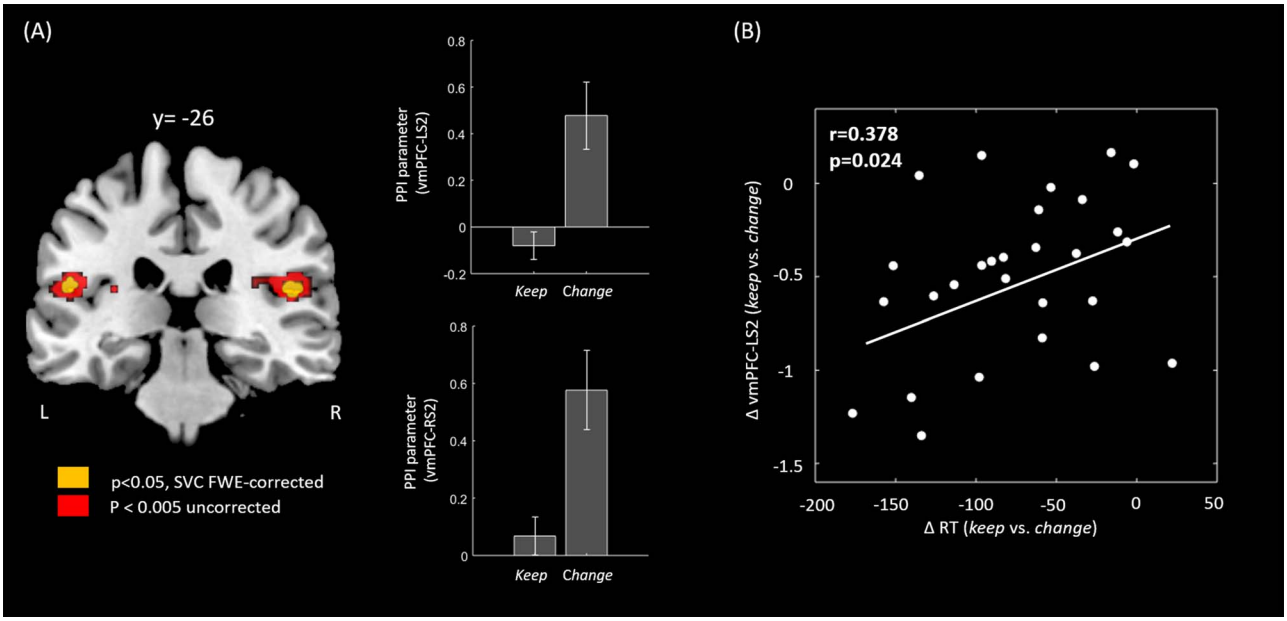


Figure 4. Connectivity between vmPFC and S2 while participants did not change their decision strategy (*Keep*) as compared with the adjustment of decision strategy (*Change*); differences in reaction times between *Keep* and *Change* were negatively correlated with changes in the connectivity strength between vmPFC and S2. (*A*) Bilateral S2 exhibited weakened connectivity with vmPFC when participants did not change their decision strategy compared with the adjustment of the decision strategy. Red = $P < 0.005$, uncorrected; yellow = $P < 0.05$, SVC, FWE-corrected. Coordinate above the coronal brain slice indexes its location in MNI space. The bar chart depicts the mean PPI parameters in bilateral S2 clusters corresponding to *Keep* and *Change* trials. The error bar depicts the standard error. (*B*) The scatterplot shows the significant correlation between changes in reaction times and functional connectivity of vmPFC and left (contralateral) S2. The weaker the connectivity between vmPFC and left S2, the faster participants indicated their decision.

### Prior Belief-Related Functional Connectivity for the Adjustment of the Decision Strategy (*Change*) and an Unchanged Decision Strategy (*Keep*)

To investigate whether functional connectivity associated with the flexibility in decision-making was modulated by prior belief across participants, we examined the relationship between the strength of individual prior belief and the strength of functional connectivity. Since the first-level three-way interaction between the physiological (i.e., BOLD signal in the seed region) and the two psychological variables (i.e., trial conditions, prior belief) did not reveal any significant results, we instead applied the gPPI data to the group-level regression analysis in SPM for *Keep* and *Change* trials separately. Regressing out the individual (mean) prior belief from *Keep* trials, we found, as expected, that the strength of prior belief significantly covaried with the connectivity strength between vmPFC and the right lateral and inferior pulvinar of the thalamus (peak MNI coordinates x/y/z = 6/−18/16, $t(1,27) = 3.98$, $P = 0.034$, small volume FWE-corrected, Fig. 5A). For *Change* trials, regression analysis revealed that the coupling between OFC and left thalamus (peak MNI coordinates x/y/z = −16/−14/10, $t(1,27) = 3.94$, $P = 0.04$, SVC, FEW-corrected, Fig. 5B) linearly decreased as the strength of prior belief increased. Corresponding activity in the thalamus was assigned to the MD and nuclei within the anterior complex. These findings largely overlapped with the results of prior belief dependent connectivity as revealed by the three-way interaction gPPI at an uncorrected threshold of $P = 0.001$ (not shown to avoid redundancies). Together, these results suggest that the stronger the participant's prior belief, the weaker the connectivity—either between vmPFC and right thalamus, if participants did not change their decision strategy, or between OFC and left thalamus, if participants adjusted their decision strategy. The same regression analysis was also applied to test for a potential relationship between the strength of connectivity and changes in reaction times. These analyses, however, revealed no significant effects, neither for *Keep* nor for *Change*.

## Discussion

Our findings suggest that different prefrontal areas relate to the flexibility in changing the decision strategy in a probabilistic environment during tactile learning. Sticking to the same decision strategy over two subsequently presented trials was associated with activity in vmPFC, whereas activity in OFC related to adjusting the decision strategy from one to the next trial. An unchanged decision strategy as compared with an updated decision strategy was associated with weakened functional connectivity between vmPFC and left S2. The connection strength between the rather cognitive-relevant vmPFC and the perception-related S2 predicted the time required to indicate the choice. If participants did not change their decision strategy, the strength of prior belief was inversely correlated with functional connectivity between vmPFC and right thalamus. If participants updated their decision strategy, the strength of prior belief was negatively correlated with functional connectivity between left OFC and left thalamus. Together, these results highlight the role of different prefrontal areas in guiding the cognitive flexibility required for decision-making during tactile learning in a probabilistic environment. Prior belief, as a key modulator of the decision strategy, appears to be related to distinct thalamo–prefrontal projections guiding successful decision-making and tactile learning.

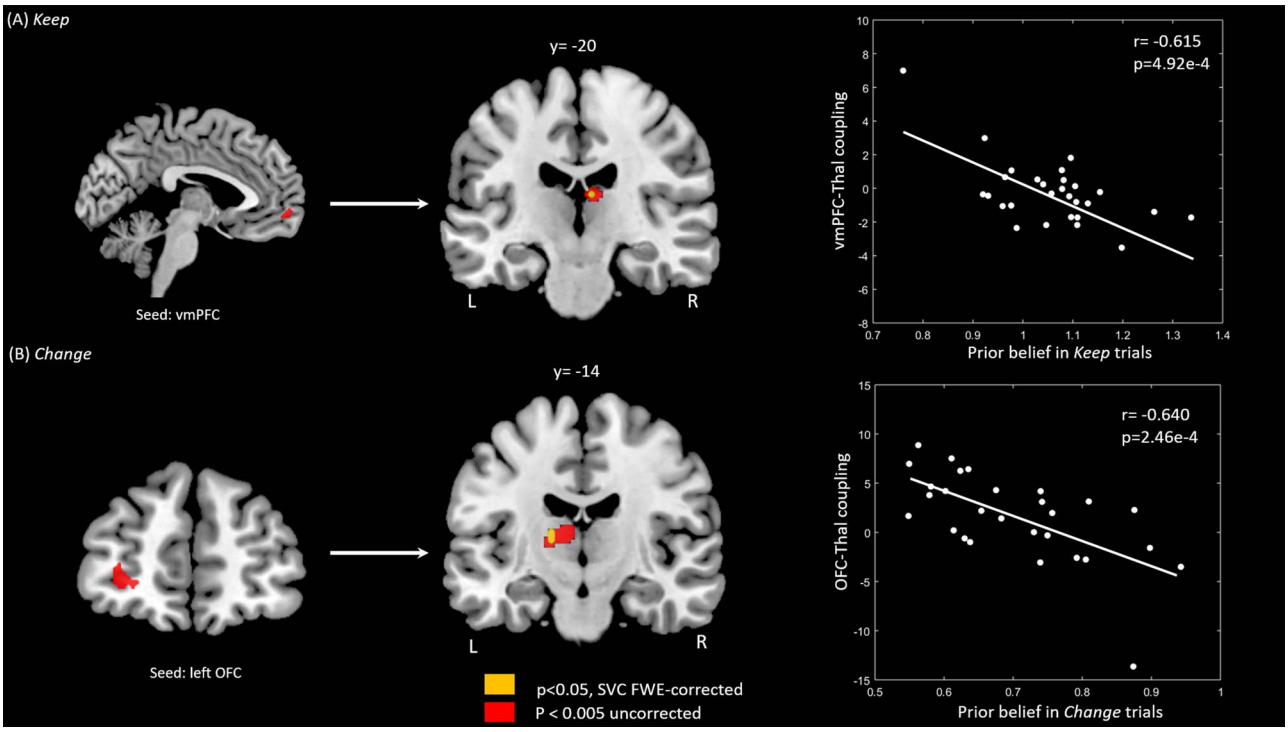


**Figure 5.** Functional connectivity between prefrontal cortex and thalamus scaled with the strength of individual prior belief. (*A*) Prior belief was inversely correlated with functional connectivity between vmPFC and left thalamus when participants did not change their decision strategy (*Keep*). (*B*) The strength of prior belief was negatively correlated with functional connectivity between OFC and right thalamus when participants updated their decision strategy (*Change*). Findings suggest that the higher prior belief, the weaker the connectivity in both conditions (*Keep* and *Change*). The seed regions are presented on sagittal and coronal brain slices for *Keep* (*A*) and *Change* (*B*), respectively (left column). Thalamic target regions are presented on coronal brain slices (middle column). Coordinates above each brain slice index their location in MNI space. Red = $P < 0.005$, uncorrected; yellow = $P < 0.05$, SVC, FWE-corrected. The scatterplots show the negative relationship between the strength of prior belief and thalamic connectivity for *Keep* and *Change*, respectively (right). The *r* and *P* values are based on a linear (Pearson) correlation analysis. They are only used to further describe the relationship between the strength of individual prior belief and thalamo–prefrontal couplings.

An unchanged decision strategy engaged the vmPFC which is a region assumed to underpin a variety of functions required for decision-making, like representing the value of a choice on the basis of past experiences (Rushworth et al. 2011; Neubert et al. 2015), or encoding the confidence for perceptual decision-making (Bang and Fleming 2018; Gherman and Philiastides 2018). Functional connectivity analyses revealed that when participants did not change their decision strategy, the coupling strength between vmPFC and S2 was weaker than for decisions that were based on an updated strategy. In monkeys, single-cell recordings from S2 neurons emphasize its role in matching past sensory experiences with present information (Romo et al. 2002). S2 and prefrontal circuits also work in concert to control decision-making and to initiate motor circuits responsible to generate the motor response (Hernández et al. 2010). Considering the representation of confidence in vmPFC and the involvement of S2 in matching past experiences with current inputs, we propose that a stronger confidence in the decision strategy (i.e., unchanged decision strategy) engages less neural processing resources, expressed by a lower connectivity strength between vmPFC and left S2. This interpretation agrees well with the theoretical accounts of the free-energy principle (Friston 2009; Friston and Kiebel 2009). This principle is based on the Bayesian idea of the brain as an inference engine. The goal is to maximize model evidence, so that surprise is minimized. Based on these principles, surprise about an unexpected target in our task may lower prior belief and model evidence and hence trigger the update of the decision strategy.

An alternative and even more likely interpretation of the involvement of vmPFC is that its activity remained unchanged for an unchanged decision strategy, so that the significant effect for *Keep* > *Change* was rather driven by vmPFC's relative deactivation when the strategy was adjusted. We cannot directly test this hypothesis, since our design was optimized to compare the conditions of interest (*Keep* and *Change*) excluding the assessment of baseline activity. The interpretation of a relative deactivation during the adjustment of the decision strategy is, nevertheless, supported by previous evidence: The vmPFC is part of the default mode network, which is most commonly active when less cognition is needed, that is, rest and mind-wandering, whereas it is deactivated when engaged in goal-oriented tasks (Buckner et al. 2008). Following this line of thought, the vmPFC–S2 connectivity could also be explained as relatively stronger coupling during the adjustment of the decision strategy as compared with an unchanged strategy. The stronger the connectivity between vmPFC and left S2, the slower participants indicated their decision during the adjustment of the decision strategy. Together, these findings suggest that prefrontal projections originating in vmPFC might propagate a kind of gating signal important for the evaluation of response options.

In relation to updating the decision strategy, we found activity in left OFC. Previous studies proposed that the OFC integrates multisensory inputs with cognitive information about stimulus history, reward, and other decision-relevant mediators to infer on the current state (Wilson et al. 2014; Schuck et al. 2016) and predict future perceptual changes (Stalnaker et al. 2014).

Primates and rodents with OFC lesions tend to stick to previously learned rules or strategies that are no longer relevant during reversal learning (Schoenbaum et al. 2002; Boulougouris et al. 2007; Clarke et al. 2008), suggesting that the OFC updates strategies during learning. These features render the OFC well suited for tracking the decision strategy throughout learning and for updating the decision strategy according to newly accumulated evidence.

The PPI analysis that accounted for the three-way interaction between the physiological (i.e., BOLD signal in the seed region) and the two psychological variables (i.e., trial conditions and prior belief) did not reveal any prior belief-associated significant results surviving FWE-corrected thresholding. This nonsignificant finding might be due to the lack of GLM efficiency in estimating three-way interactions if combined with conservative FWE thresholding. Applying an uncorrected threshold at $P = 0.001$ largely resembled the findings of the group-level multiple linear regression analysis, which supports its validity. The group-level multiple linear regression analysis revealed that the strength of prior belief appeared to be significantly related to two distinct thalamo–prefrontal pathways.

Recently, evidence has emerged assigning the thalamus a central role in cognitive processes underpinning, for instance, learning (Mitchell 2015; Yamanaka et al. 2018), memory (Van Groen et al. 2002), attention (De Bourbon-Teles et al. 2014; Wright et al. 2015), and decision-making (Mitchell 2015; Chakraborty et al. 2019). The right thalamic cluster, involved in encoding the strength of individual prior belief through connections with vmPFC for an unchanged decision strategy, overlapped with the lateral and inferior pulvinar, whereas the left thalamic region, involved in updating the decision strategy through connections to the OFC, was located in the MD and nuclei within the anterior complex (Behrens et al. 2003). Both pulvinar and MD are considered to represent a sort of "higher order thalamic relays" that are reciprocally interconnected to associated cortical targets via cortico–thalamo–cortical connections (Guillery, 1995). The pulvinar seems to play an important role in visual processing and attentional calibration processes (Grieve et al. 2000; Bridge et al. 2016). Previous evidence emphasizes that MD is also involved in learning new object–reward associations as compared with the retention and retrieval of previously acquired information (Mitchell et al. 2008; Mitchell and Gaffan 2008). Projections from the medial prefrontal cortex to the midline thalamic nucleus seem to underpin the encoding of reward-predictive cues (Otis et al. 2017) and general behavioral flexibility (Nakayama et al. 2018), particularly during rapid trial-by-trial associative learning and decision-making demanding rule switching (Mitchell 2015; Marton et al. 2018). MD and OFC were shown to work in concert to update action–outcome associations during reversal learning (Parnaudeau et al. 2018; Fresno et al. 2019), which is in-line with our finding of an association with updating the decision strategy. Given that the thalamus comprises many nuclei, each with different connectivity and functional properties, our findings emphasize the notion that distinct thalamic subregions play multifaceted roles in guiding the flexibility in decision-making through tight interactions with various prefrontal cortices. Notably, prior belief and reaction time may be represented by partly different prefrontal networks, since there was no direct (linear) relationship between these measures. Accordingly, prior belief may be constituted by accumulated evidence about the current state of the environment as derived from past experiences, whereas reaction time may rather reflect perceptual processing and the initiation of the motor response.

Taken together, present findings advance our understanding of the thalamus as a crucial mediator of the flexibility in changing or keeping the decision strategy via communication with prefrontal regions during probabilistic learning. Future research should broaden the focus on related decision modulators, like reward and punishment, and how the thalamus, as a potential gate for decision-making, integrates corresponding information (Campus et al. 2019).

## Supplementary Material

Supplementary material is available at *Cerebral Cortex* online.

## Funding

Deutsche Forschungsgemeinschaft (DFG, German Research Foundation): Project number 122679504—SFB 874 "Integration and Representation of Sensory Processes."

*Conflict of Interest*: The authors declare no competing financial interests.

## References

Allen M, Fardo F, Dietz MJ, Hillebrandt H, Friston KJ, Rees G, Roepstorff A. 2016. Anterior insula coordinates hierarchical processing of tactile mismatch responses. *Neuroimage*. 127:34–43.

Ashburner J, Friston KJ. 2005. Unified segmentation. *Neuroimage*. 26:839–851.

Bang D, Fleming SM. 2018. Distinct encoding of decision confidence in human medial prefrontal cortex. *Proc Natl Acad Sci U S A*. 115:6082–6087.

Bari BA, Grossman CD, Lubin EE, Rajagopalan AE, Cressy JI, Cohen JY. 2019. Stable representations of decision variables for flexible behavior. *Neuron*. 103:922–933.

Behrens TEJ, Johansen-Berg H, Woolrich MW, Smith SM, Wheeler-Kingshott CAM, Boulby PA, Barker GJ, Sillery EL, Sheehan K, Ciccarelli O *et al.* 2003. Non-invasive mapping of connections between human thalamus and cortex using diffusion imaging. *Nat Neurosci*. 6:750–757.

Behrens TEJ, Woolrich MW, Walton ME, Rushworth MFS. 2007. Learning the value of information in an uncertain world. *Nat Neurosci*. 10:1214–1221.

Bestmann S, Harrison LM, Blankenburg F, Mars RB, Haggard P, Friston KJ, Rothwell JC. 2008. Influence of uncertainty and surprise on human corticospinal excitability during preparation for action. *Curr Biol*. 18:775–780.

Boulougouris V, Dalley JW, Robbins TW. 2007. Effects of orbitofrontal , infralimbic and prelimbic cortical lesions on serial spatial reversal learning in the rat. *Behav Brain Res*. 179:219–228.

Bridge H, Leopold DA, Bourne JA. 2016. Adaptive Pulvinar circuitry supports visual cognition. *Trends Cogn Sci*. 20:146–157.

Buckner RL, Andrews-Hanna JR, Schacter DL. 2008. The brain's default network: anatomy, function, and relevance to disease. *Ann N Y Acad Sci*. 1124:1–38.

Campus P, Covelo IR, Kim Y, Parsegian A, Kuhn BN, Lopez SA, Neumaier JF, Ferguson SM, Solberg Woods LC, Sarter M *et al.* 2019. The paraventricular thalamus is a critical mediator of top-down control of cue-motivated behavior in rats. *Elife*. 8:1–25.

Chakraborty S, Ouhaz Z, Mason S, Mitchell AS. 2019. Macaque parvocellular mediodorsal thalamus: dissociable contributions to learning and adaptive decision-making. *Eur J Neurosci*. 49:1041–1054.

Clark A. 2013. Whatever next? Predictive brains, situated agents, and the future of cognitive science. *Behav Brain Sci*. 36:181–204.

Clarke HF, Robbins TW, Roberts AC. 2008. Lesions of the medial striatum in monkeys produce perseverative impairments during reversal learning similar to those produced by lesions of the orbitofrontal cortex. *J Neurosci*. 28:10972–10982.

De Bourbon-Teles J, Bentley P, Koshino S, Shah K, Dutta A, Malhotra P, Egner T, Husain M, Soto D. 2014. Thalamic control of human attention driven by memory and learning. *Curr Biol*. 24:993–999.

den Ouden HEM, Daunizeau J, Roiser J, Friston KJ, Stephan KE. 2010. Striatal prediction error modulates cortical coupling. *J Neurosci*. 30:3210–3219.

Dreher J-C, Schmidt PJ, Kohn P, Furman D, Rubinow D, Berman KF. 2007. Menstrual cycle phase modulates reward-related neural function in women. *Proc Natl Acad Sci*. 104:2465–2470.

Eickhoff SB, Stephan KE, Mohlberg H, Grefkes C, Fink GR, Amunts K, Zilles K. 2005. A new SPM toolbox for combining probabilistic cytoarchitectonic maps and functional imaging data. *Neuroimage*. 25:1325–1335.

Fardo F, Auksztulewicz R, Allen M, Dietz MJ, Roepstorff A, Friston KJ. 2017. Expectation violation and attention to pain jointly modulate neural gain in somatosensory cortex. *Neuroimage*. 153:109–121.

Fresno V, Parkes SL, Faugère A, Coutureau E, Wolff M. 2019. A thalamocortical circuit for updating action-outcome associations. *Elife*. 8:e46187.

Friston K. 2005. A theory of cortical responses. *Philos Trans R Soc B Biol Sci*. 360:815–836.

Friston K. 2009. The free-energy principle: a rough guide to the brain? *Trends Cogn Sci*. 13:293–301.

Friston K, Kiebel S. 2009. Predictive coding under the free-energy principle. *Philos Trans R Soc B Biol Sci*. 364:1211–1221.

Friston KJ, Buechel C, Fink GR, Morris J, Rolls E, Dolan RJ. 1997. Psychophysiological and modulatory interactions in neuroimaging. *Neuroimage*. 6:218–229.

Gherman S, Philiastides MG. 2018. Human VMPFC encodes early signatures of confidence in perceptual decisions. *Elife*. 7:e38293.

Guillery RW. 1995. Anatomical evidence concerning the role of the thalamus in corticocortical communication: a brief review. *J Anat*. 187:583–592.

Grieve KL, Acuña C, Cudeiro J. 2000. The primate pulvinar nuclei: vision and action. *Trends Neurosci*. 23(1):35–39.

Hernández A, Nácher V, Luna R, Zainos A, Lemus L, Alvarez M, Vázquez Y, Camarillo L, Romo R. 2010. Decoding a perceptual decision process across cortex. *Neuron*. 66:300–314.

Howard JD, Kahnt T, Gottfried JA. 2016. Converging prefrontal pathways support associative and perceptual features of conditioned stimuli. *Nat Commun*. 7:11546.

Iglesias S, Mathys C, Brodersen KH, Kasper L, Piccirelli M, DenOuden HEM, Stephan KE. 2013. Hierarchical prediction errors in midbrain and basal forebrain during sensory learning. *Neuron*. 80:519–530.

Kuhns AB, Dombert PL, Mengotti P, Fink GR, Vossel S. 2017. Spatial attention, motor intention, and Bayesian cue predictability in the human brain. *J Neurosci*. 37:5334–5344.

Marton TF, Seifikar H, Luongo FJ, Lee AT, Sohal VS. 2018. Roles of prefrontal cortex and mediodorsal thalamus in task engagement and behavioral flexibility. *J Neurosci*. 38:2569–2578.

Mathys C, Daunizeau J, Friston KJ, Stephan KE. 2011. A bayesian foundation for individual learning under uncertainty. *Front Hum Neurosci*. 5:39.

McLaren DG, Ries ML, Xu G, Johnson SC. 2012. A generalized form of context-dependent psychophysiological interactions (gPPI): a comparison to standard approaches. *Neuroimage*. 61:1277–1286.

Mitchell AS. 2015. The mediodorsal thalamus as a higher order thalamic relay nucleus important for learning and decision-making. *Neurosci Biobehav Rev*. 54:76–88.

Mitchell AS, Browning PGF, Wilson CRE, Baxter MG, Gaffan D. 2008. Dissociable roles for cortical and subcortical structures in memory retrieval and acquisition. *J Neurosci*. 28:8387–8396.

Mitchell AS, Gaffan D. 2008. The magnocellular mediodorsal thalamus is necessary for memory acquisition, but not retrieval. *J Neurosci*. 28:258–263.

Nakayama H, Ibañez-Tallon I, Heintz N. 2018. Cell-type-specific contributions of medial prefrontal neurons to flexible behaviors. *J Neurosci*. 38:4490–4504.

Neubert FX, Mars RB, Sallet J, Rushworth MFS. 2015. Connectivity reveals relationship of brain areas for reward-guided learning and decision making in human and monkey frontal cortex. *Proc Natl Acad Sci U S A*. 112:E2695–E2704.

Otis JM, Namboodiri VMK, Matan AM, Voets ES, Mohorn EP, Kosyk O, McHenry JA, Robinson JE, Resendez SL, Rossi MA *et al*. 2017. Prefrontal cortex output circuits guide reward seeking through divergent cue encoding. *Nature*. 543:103–107.

Parnaudeau S, Bolkan SS, Kellendonk C. 2018. The Mediodorsal thalamus: an essential partner of the prefrontal cortex for cognition. *Biol Psychiatry*. 83:648–656.

Preuschoff K, Bossaerts P. 2007. Adding prediction risk to the theory of reward learning. *Ann N Y Acad Sci*. 1104:135–146.

Rescorla R, Wagner A. 1972. A theory of Pavlovian conditioning: variations in the effectiveness of reinforcement and nonreinforcement. In: Black AH & Prokasy W.F., editors. *Classical conditioning II: current research and theory*. New York: Appleton-Century-Crofts, pp. 64–99.

Romo R, Hernández A, Zainos A, Lemus L, Brody CD. 2002. Neuronal correlates of decision-making in secondary somatosensory cortex. *Nat Neurosci*. 5:1217–1225.

Rushworth MFS, Noonan MAP, Boorman ED, Walton ME, Behrens TE. 2011. Frontal cortex and reward-guided learning and decision-making. *Neuron*. 70:1054–1069.

Sacher J, Okon-Singer H, Villringer A. 2013. Evidence from neuroimaging for the role of the menstrual cycle in the interplay of emotion and cognition. *Front Hum Neurosci*. 7:1–7.

Schoenbaum G, Nugent CASL, Saddoris MP, Setlow B. 2002. Orbitofrontal lesions in rats impair reversal but not acquisition of go, no-go odor discriminations. *Neuroreport*. 13:885–890.

Schuck NW, Cai MB, Wilson RC, Niv Y. 2016. Human orbitofrontal cortex represents a cognitive map of state space. *Neuron*. 91:1402–1412.

Seth AK. 2013. Interoceptive inference, emotion, and the embodied self. *Trends Cogn Sci*. 17:565–573.

Seth AK, Suzuki K, Critchley HD. 2012. An interoceptive predictive coding model of conscious presence. *Front Psychol*. 2:395.

Stalnaker TA, Cooch NK, McDannald MA, Liu TL, Wied H, Schoenbaum G. 2014. Orbitofrontal neurons infer the value and identity of predicted outcomes. *Nat Commun*. 5:3926.

van Ede F, Jensen O, Maris E. 2010. Tactile expectation modulates pre-stimulus beta-band oscillations in human sensorimotor cortex. *Neuroimage*. 51:867–876.

van Ede F, Szebényi S, Maris E. 2014. Attentional modulations of somatosensory alpha, beta and gamma oscillations dissociate between anticipation and stimulus processing. *Neuroimage*. 97:134–141.

Van Groen T, Kadish I, Wyss JM. 2002. The role of the laterodorsal nucleus of the thalamus in spatial learning and memory in the rat. *Behav Brain Res*. 136:329–337.

Vossel S, Bauer M, Mathys C, Adams RA, Dolan RJ, Stephan KE, Friston KJ. 2014. Cholinergic stimulation enhances Bayesian belief updating in the deployment of spatial attention. *J Neurosci*. 34:15735–15742.

Vossel S, Mathys C, Stephan KE, Friston KJ. 2015. Cortical coupling reflects Bayesian belief updating in the deployment of spatial attention. *J Neurosci*. 35:11532–11542.

Wang BA, Schlaffke L, Pleger B. Forthcoming 2020. Modulations of insular projections by prior belief mediate the precision of prediction error during tactile learning. *J Neurosci*.

Weilnhammer VA, Stuke H, Sterzer P, Schmack K. 2018. The neural correlates of hierarchical predictions for perceptual decisions. *J Neurosci*. 38:5008–5021.

Wetherill RR, Jagannathan K, Hager N, Maron M, Franklin TR. 2016. Influence of menstrual cycle phase on resting-state functional connectivity in naturally cycling, cigarette-dependent women. *Biol Sex Differ*. 7:1–9.

Wilson RC, Takahashi YK, Schoenbaum G, Niv Y. 2014. Orbitofrontal cortex as a cognitive map of task space. *Neuron*. 81:267–279.

Wright NF, Vann SD, Aggleton JP, Nelson AJD. 2015. A critical role for the anterior thalamus in directing attention to task-relevant stimuli. *J Neurosci*. 35:5480–5488.

Yamanaka K, Hori Y, Minamimoto T, Yamada H, Matsumoto N, Enomoto K, Aosaki T, Graybiel AM, Kimura M. 2018. Roles of centromedian parafascicular nuclei of thalamus and cholinergic interneurons in the dorsal striatum in associative learning of environmental events. *J Neural Transm*. 125: 501–513.

Zaborszky L, Hoemke L, Mohlberg H, Schleicher A, Amunts K, Zilles K. 2008. Stereotaxic probabilistic maps of the magnocellular cell groups in human basal forebrain. *Neuroimage*. 42:1127–1141.